Biogeosciences Discuss., 10, 16405–16452, 2013
www.biogeosciences-discuss.net/10/16405/2013/
doi:10.5194/bgd-10-16405-2013
© Author(s) 2013. CC Attribution 3.0 License.

Biogeosciences
Discussions
Open Access

This discussion paper is/has been under review for the journal Biogeosciences (BG).
Please refer to the corresponding final paper in BG if available.

Discussion Paper | Discussion Paper | Discussion Paper | Discussion Paper |

Mixed layer variability and chlorophyll *a* biomass in the Bay of Bengal

J. Narvekar and S. Prasanna Kumar

CSIR-National Institute of Oceanography, Dona Paula, Goa 403 004, India

Received: 3 September 2013 – Accepted: 11 September 2013 – Published: 24 October 2013

Correspondence to: S. Prasanna Kumar (prasanna@nio.org)

Published by Copernicus Publications on behalf of the European Geosciences Union.

Abstract

Mixed layer is the most variable and dynamically active part of the marine environment that couples the underlying ocean to the atmosphere and plays an important role in determining the chlorophyll concentration. In this paper we examined the seasonal variability of the mixed layer depth in the Bay of Bengal, the factors responsible for it and the coupling of mixed layer processes to the chlorophyll biomass using a suite of in situ as well as remote sensing data. The basin-wide mixed layer depth was the shallowest during spring intermonsoon, which was associated with strong themohaline stratification of the upper water column. The prevailing winds which were the weakest of all the seasons were unable to break the stratification leading to the observed shallow mixed layer. Consistent with the warm oligotrophic upper ocean, the surface chlorophyll concentrations were the least and the vertical profile of chlorophyll was characterized by a subsurface chlorophyll maximum. Similarly, during summer though the monsoon winds were the strongest they were unable to break the upper ocean haline-stratification in the northern Bay brought about by a combination of excess precipitation over evaporation and fresh water influx from rivers adjoining the Bay of Bengal. Consistent with this though the nitrate concentrations were high in the northern part of the Bay, the chlorophyll concentrations were low indicating the light limitation. In contrast, in the south, advection of high salinity waters from the Arabian Sea coupled with the westward propagating Rossby waves of annual periodicity were able to decrease stability of the upper water column and the prevailing monsoon winds were able to initiate deep mixing leading to the observed deep mixed layer. The high chlorophyll concentration observed in the south resulted from the positive wind stress curl which pumped nutrient rich subsurface waters to the euphotic zone. The southward extension of the shallow mixed layer in fall intermonsoon resulted from the advection of low salinity waters from the northern Bay combined with the secondary heating by the incoming short wave radiation. The satellite-derived chlorophyll pigment concentration during fall intermonsoon was similar to that of summer but with reduced values. The basin-wide deep

BGD

10, 16405–16452, 2013

cc BY

mixed layer during winter resulted from a combination of reduced short wave radiation, increase in salinity and comparatively stronger winds. The mismatch between the low nitrate and comparatively higher chlorophyll biomass during winter indicated the efficacy of the limited nitrate data to adequately resolve the coupling between the mixed layer processes and the chlorophyll biomass.

1 Introduction

The upper ocean experiences large spatio-temporal variability compared to the rest of the ocean and hence it forms an important region for understanding both short-term and long-term changes including climate change. The intense mixing in the upper ocean by heat, momentum and freshwater flux results in the formation of a homogeneous layer with nearly-uniform properties known as mixed layer. It is this layer that couples the underlying ocean to the atmosphere through the transfer of mass and energy. The heat stored in the mixed layer regulates the air-sea exchange processes including convection and cyclone genesis. In addition, bulk of the oceanic biological productivity critically depends on the physical and chemical changes taking place within this layer. Spatially the mixed layer thickness increases from few tens of meters at the equator to few hundreds of meter at the poles (Monterey and Levitus, 1997), while temporally it could vary from diurnal to inter-annual time scales (Weller and Farmer, 1992; Brainerd and Gregg, 1995; Kara et al., 2003). However, within a given geographical region, such as tropics, the structure and variability of mixed layer largely depends on the regional oceanographic characteristics and atmospheric forcing.

The Bay of Bengal situated in the eastern part of the northern Indian Ocean is a tropical basin, which is landlocked in the north and is forced by semi-annually reversing monsoon wind system. The strongest winds occur during summer monsoon (June–September) when the southwesterly winds bring humid maritime air mass into the Bay of Bengal. In contrast, during winter monsoon (November–February), the winds are weak and from northeasterly direction. These northeast trade winds bring cool and

BGD
10, 16405–16452, 2013

CC BY

dry continental air mass to the Bay of Bengal. The unique feature of the Bay of Bengal is the large seasonal freshwater influx from rivers ($1.625 \times 10^{12}\,m^3\,yr^{-1}$, Subramanian, 1993) as well as excess precipitation over evaporation ($\sim 2\,m\,yr^{-1}$, Prasad, 1997), which makes the waters of the upper layers less saline and highly stratified. This fresh water input leads to the formation of strong halocline within the upper isothermal layer known as "barrier layer" (Lukas and Linderstrom, 1991; Sprintall and Tomczak, 1992).

In the past several studies attempted to understand the mixed layer variability in the Indian Ocean including Bay of Bengal. There exist a few climatologies of the mixed layer depth for the tropical Indian Ocean (Colborn, 1975; Robinson et al., 1979; Levitus, 1982; Hastenrath and Greisher, 1989; Rao et al., 1989). Based on the time series data collected during MONSOON-77 and MONEX-79, Gopalakrishna et al. (1988) studied the influence of wind on the variability of the mixed layer in the northern Indian Ocean during different phases of summer monsoon. Using global ocean temperature climatology, Rao and Sivakumar (2000) studied the near surface thermal structure and heat budget of the mixed layer of the tropical Indian Ocean including Bay of Bengal. Han et al. (2001) showed that in the regions where precipitation exceeds evaporation the mixed layer was found to be thin because of decreased entrainment and increased barrier layer. While comparing the total kinetic energy available for mixing in the Arabian Sea and the Bay of Bengal, Shenoi et al. (2002) stated that the shallow mixed layer depth in the Bay of Bengal during the summer monsoon is primarily driven by a combination of weaker winds and strong near-surface stratification. Subsequently, Vinaychandran et al. (2002) argued that strong stratification associated with the barrier layer curtails the vertical mixing leading to the formation of shallow mixed layers. In contrast, with help of one dimensional turbulent closure model Prasad (2004) studied the physical mechanism governing the seasonal evolution of mixed layer depth along two transects along the central Arabian Sea and Bay of Bengal and concluded that the surface forcing controls mixed layer depth in the Bay of Bengal rather than the vertical salinity stratification. Influence of salinity on the seasonal evolution of mixed layer in the Bay of Bengal was studied by Rao and Sivakumar (2003) using climatological data.

BGD
10, 16405–16452, 2013

CC BY

Narvekar and Prasanna Kumar (2006) examined the seasonal cycle of mixed layer in the central Bay of Bengal and its association to chlorophyll using more comprehensive data set including Argo data. Using global general circulation model De Boyer Montegut et al. (2007) studied the mixed layer heat budget of the Bay of Bengal as a part of northern Indian Ocean and stated that the salinity stratification plays a clear role in maintaining a high winter SST in the Bay of Bengal while presence of freshwater near the surface allows heat storage below the surface layer that can later be recovered by entrainment warming during winter cooling. More recently, Keerthi et al. (2012) studied the inter-annual variability of the mixed layer in the tropical Indian Ocean and its link to climate modes using eddy permitting numerical simulation and in situ hydrographic data.

All of the above studies examined the variability of the mixed layer in the context of wind-mixing, net heat flux and fresh water flux. Most of them used monthly mean climatlogy of in situ data to address the mixed layer variability over Indian Ocean of which Bay of Bengal forms a part. The rest of the study used in situ data collected from a limited spatial and temporal coverage in the Bay of Bengal during a particular cruise. Though the above studies yielded a fairly good understanding of the processes controlling the mixed layer variability in the Bay of Bengal, there are several aspects which are yet to be addressed such as role of advection and remote forcing. More importantly, we do not yet understand with sufficient details the role of mixed layer in regulating the basin-wide variability in chlorophyll biomass and primary productivity. It is in this context that the present paper attempts to understand (1) processes controlling basin-wide variability of the mixed-layer and (2) coupling between mixed layer and chlorophyll biomass in the Bay of Bengal on a seasonal scale. In the present study using a more comprehensive quality-controlled hydrographic data and atmospheric data we explore the role of local forcing via heat, momentum and fresh water fluxes and remote forcing via propagating waves and advection of high salinity waters from the Arabian Sea in controlling mixed layer variability on seasonal time-scale and its coupling to the chlorophyll biomass.

BGD
10, 16405–16452, 2013

J. Narvekar and S. Prasanna Kumar

CC BY

2 Data and methodology

In order to study the seasonal variability of mixed layer in the Bay of Bengal in response to the local and remote forcing and its coupling to basin-scale distribution of chlorophyll, a suite of both in-situ and remote sensing data pertaining to oceanographic and atmospheric parameters were used. The domain within which both the oceanographic and meteorological data extracted were for the region equator to 25° N latitude and 75° to 100° E longitude.

2.1 Hydrographic data

The hydrographic data pertaining to temperature and salinity was extracted from the following 3 sources:

1. The World Ocean Data base 2005 (WOD05) (Boyer et al., 2006) contained temperature and salinity data from Hydro-cast for the period 1919 to 2000 and conductivity temperature-depth (CTD) profiles for the period 1972 to 2003 (http://www.nodc.noaa.gov/OC5/WOD05/pr_wod05.html).

2. Responsible National Oceanographic Data Center (RNODC) at National Institute of Oceanography (CSIR-NIO), Goa which contained temperature and salinity data from Hydro-cast for the period 1972–1996 and CTD profiles for the period 1979–2006. All the data were collected on board Indian research ships.

3. Argo data which contained the temperature and salinity profiles for the period 2002 to 2007 were extracted from http://www.usgodae.org/argo/argo.html.

In all 7197 profiles of temperature and salinity from Hydro-cast, 2714 profiles from CTD and 4569 profiles from Argo were extracted. These profiles were subjected to the following quality control procedures to obtain quality data for further analysis.

At first all the profiles with depth less than 50 m were eliminated, as the objective of the study was to determine mixed layer depth, which may exceed 50 m. The remaining

CC BY

data were physically examined and duplicate profiles as well as those with obvious errors were excluded. After the quality control, the total number of Hydro-cast profiles was reduced to 5328 (882 RNODC & 4446 WOD05), CTD profiles to 2656 (1803 RNODC & 853 WOD05) and Argo profiles to 4203. From the quality checked data the spatial distribution of total number of temperature and salinity profiles available on a 1° latitude by 1° longitude grids is presented in Fig. 1, while total number of profiles for each month is given in Table 1. From the quality-controlled temperature and salinity profiles, density (sigma-*t*) was calculated (UNESCO, 1981) up to a depth of 500 m. This data was further used to prepare monthly mean climatology of temperature, salinity and sigma-*t* on a 1° latitude by 1° longitude grids. These profiles were used to determine mixed layer depth (MLD).

In order to determine the mixed layer depth one could either specify a difference in temperature or density (sigma-*t*) from the surface value (Wyrtki, 1964; Levitus, 1982; Schneider and Muller, 1990) or specify a gradient in temperature or density (sigma-*t*) (Bathen, 1972; Lukas and Lindstrom, 1991) depending upon the vertical structure of temperature, salinity and sigma-*t* of the region. An examination of the vertical profiles of temperature, salinity and density (sigma-*t*) at two locations representing the northern (19° N, 89° E) and southern (9° N, 89° E) Bay of Bengal during February (winter) and August (summer) showed that in the southern part of the Bay of Bengal the isothermal, isohaline and isopycnal layers, in general, coincided in the upper ocean irrespective of the season (Fig. 2 left panels). In the northern part of the Bay of Bengal there was practically no isohaline layer in the vertical profile of salinity and the salinity rapidly increased within the isothermal layer (Fig. 2 right panels). However, at times the salinity profile showed a thin isohaline layer in the upper water column (not shown). In view of the above, in the present study we defined MLD as the depth at which the density (sigma-*t*) exceeds the surface value by 0.2 kg m^{-3}. The monthly mean temperature, salinity and density (sigma-*t*) profiles were interpolated on to 1 m depth interval by using cubic spline method and MLD was determined numerically. The temperature and

BGD
10, 16405–16452, 2013

salinity data was further used for the computation of static stability parameter following Pond and Pickard (1983)

$$E = -\frac{1}{\rho}\frac{\partial \rho}{\partial z} \qquad (1)$$

where E is the static stability parameter (m^{-1}), ρ is the density ($kg\,m^{-3}$) of the water and z is the depth (m).

2.2 Nitrate and chlorophyll *a* data

The nitrate profiles for the present study were obtained from the World Ocean Data base 2005 (WOD05) and RNODC. The former contained the nitrate data for the period 1906–1999 while latter had the data for the period 1973–2006. The total number of nitrate profiles extracted from the above sources was 7406. From these the duplicate profiles were removed first and then the rest of the profiles were physically checked for any obvious ambiguity, which was removed subsequently. The quality control procedure reduced the total number of profiles to 2653. The number of profiles available at each of the 1° latitude × 1° longitude grid is shown in Fig. 3a.

The chlorophyll *a* profiles were taken from RNODC, which contained data for the period 1951–2006. The total number of chlorophyll *a* profiles was 1060 and after the quality control procedure, similar to that of nitrate, the number of profiles reduced to 1030. The number of chlorophyll *a* profiles available in each of the 1° latitude × 1° longitude grid was shown in Fig. 3b.

Since the total number of nitrate and chlorophyll *a* profiles in each of the one-degree grid itself was less, these data were grouped together in time to produce seasonal climatology. The seasons considered for this purpose were defined as:

- Spring intermonsoon March–May
- Summer monsoon June–August

BGD
10, 16405–16452, 2013

J. Narvekar and S. Prasanna Kumar

CC BY

– Fall intermonsoon September–October

– Winter monsoon November–February

Since spatial coverage of data during fall intermonsoon was very poor and was confined to western Bay of Bengal, this season was not considered.

2.3 River runoff data

The monthly mean climatology of river discharge of 6 major rivers Ganges, Brahmaputra, Irrawady, Godavari, Krishna and Cauvery were taken from Global Runoff data Centre, Germany (http://grdc.bafg.de/servlet/is/2781).

2.4 Atmospheric data

Meteorological data were extracted from the National Oceanographic Centre (NOC), Southampton, climatology (formerly Southampton Oceanographic Centre, SOC) (http://www.noc.soton.ac.uk/ooc/CLIMATOLOGY/noc11.php) in the study domain (0–25° N and 75–100° E) for the period from 1980 to 2005. It contained the monthly mean climatology of incoming short wave radiation, wind speed, evaporation, precipitation and net heat flux on 1° longitude by 1° latitude grid.

2.5 Remote sensing data

Since the in situ chlorophyll data was limited in both space and time, chlorophyll pigment concentrations derived from global 9 km monthly mean imagery of Sea-viewing Wide Field-of-view Sensor (SeaWiFS) for the period September 1997 to December 2007 was used (http://reason.gsfc.nasa.gov/OPS/Giovanni/ocean.seawifs.shtml). From these data the climatological seasonal means were calculated for spring intermonsoon, summer monsoon, fall intermonsoon and winter monsoon.

Merged sea-level anomalies of Topex/Poseidon ERS1/2 series satellites obtained from AVISO live access server (http://las.aviso.oceanobs.com) was also used for the

BGD
10, 16405–16452, 2013

CC BY

period October 1992 to January 2006, which gives 7 day snapshots having a spatial resolution of 1/3rd of a degree, to prepare monthly mean climatology of sea-level anomaly. From the sea-level height anomalies, velocities were computed assuming the geostrophic relation (Pond and Pickard, 1983)

$$2\Omega \sin(\varphi) \cdot V = g \tan(i) \tag{2}$$

where Ω is the earth's angular velocity, φ is the latitude, V is the velocity and tan(i) is the slope of the sea surface.

3 Results and discussion

We first examined the spatio-temporal variability of mixed layer depth (MLD) by analyzing the monthly mean climatology. To understand the processes affecting the mixed layer variability we examined the monthly mean climatology of sea surface temperature (SST), sea surface salinity (SSS), incoming short wave radiation, net heat flux (NHF), wind speed (WS), momentum flux (wind-stress curl) and the fresh water flux (evaporation-precipitation; E-P) in tandem with MLD. For brevity we have presented the monthly mean climatology of all the above parameters in the Appendix. In the main text we present the monthly mean climatology of MLD superimposed with relevant parameters that are responsible for the observed variability in the mixed layer and discussed the seasonal cycle. Finally, we examine the seasonal variability of chlorophyll and nutrient to understand the possible link between them and mixed layer.

3.1 Spring intermonsoon

The mixed layer depth during spring intermonsoon (March-April-May; Fig. 4a–c) was the shallowest in the Bay of Bengal compared to the rest of the months (Appendix Fig. A1), particularly during March and April. It varied between 10 and 25 m except in the southwestern region in March and April and near the western boundary in April.

CC BY

In May, however, the shallow MLD was confined to the region north of 16° N (Fig. 4c). Another region of comparatively shallow MLD (~ 25 m) was seen in a band between 6° and 9° N encompassing peninsular India and Sri Lanka. The rest of the basin, however, showed slightly deeper MLD (30–35 m).

The observed MLD variability could be understood in the light of the prevailing ocean-atmospheric conditions. The incoming solar radiation peaked during March–April (280–290 $W m^{-2}$, Fig. A4) with a corresponding peak in the net heat flux (150–160 $W m^{-2}$, Fig. A5). The basin-wide winds were the weakest during this period (4–5 $m s^{-1}$, Fig. A6), except near the western boundary in April where a core of high wind speed as well as negative wind stress curl was noticed (Fig. 4b). Note that the peak solar heating and subsequent highest net heat gain by the ocean lead to thermal stratification. In addition, low salinity waters in the northern Bay (north of 18° N) with salinity less than 32.5 psu (Fig. A3) during March–April lead to strong haline stratification, specially the upper 20 m, as is evident from the vertical profiles of the stability parameter (Fig. 4d). Thus, during spring Intermonsoon the weak winds were unable to break the strong thermohaline stratification to drive deep wind-mixing and hence led to the formation of shallow mixed layer.

In the south, comparatively deeper mixed layer (~ 35 m) seen west of 90° E appears to be linked to the prevailing salinity and wind conditions. The presence of relatively high salinity waters (> 34.5 psu) during spring Intermonsoon (Fig. A3) made the upper water column, specially the upper 30 m, less stable compared to north (Fig. 4d) and the moderate winds (Fig. A6) were able to initiate greater mixing which lead to the observed deep MLD. The comparatively deeper MLD along the western boundary (> 25 m) in April was driven by the strong negative wind stress curl ($\sim -20 \times 10^{-8}$ Pascal m^{-1}, Fig. 4b). However, the comparatively shallow MLD in a band between 6° and 10° N east of Sri Lanka and southern tip of India during April–May cannot be explained in the context of the prevailing ocean atmospheric condition alone and hence we have examined the role of planetary waves such as Rossby waves in a separate section.

BGD
10, 16405–16452, 2013

cc BY

3.2 Summer monsoon

Mixed layer during summer monsoon (June-July-August) was the deepest. With the progress of summer monsoon from June to August the mixed layer in most parts of the Bay and in the region between equator and 6° N was deep (Fig. 5a–c). However, along the western boundary and in the northern and eastern part of the Bay MLD was shallow. Similarly, the region around peninsular India and Sri Lanka also showed the presence of shallow mixed layer. With the progress of summer monsoon, the region of shallow mixed layer around Sri Lanka showed a progressive eastward extension with time. The observed pattern of MLD variation could be explained in the following manner. Though the wind speeds were the highest during summer monsoon in the entire basin (Fig. A6), the MLD were the shallowest in the northern Bay (< 10 m). An examination of *E*-*P* showed that it was negative and the highest of all the season, implying excess precipitation, in excess of 440 mm month^{-1}, in the northern Bay (Fig. A8). In addition to the oceanic precipitation, the influx of freshwaters from the rivers adjoining the Bay of Bengal also contributes towards freshening of the surface waters of the Bay. An examination of the monthly mean climatology of river discharge of 5 major rivers Ganges, Brahmaputra, Irrawady, Godavari, and Krishna showed that the freshwater discharge dominated during July to October (Fig. 5d). The spreading of low salinity waters (< 32 psu) were seen from the northern Bay towards the south and also along eastern and western boundary (see the blue cross-hatch in Fig. 5a–c) with the progress of summer monsoon. Note that the upper ocean was very warm with SST in excess of 28.5 °C (Fig. A2). These warm and low salinity waters contributed towards strengthening the stratification of the upper ocean as could be inferred from the stability parameter (Fig. 5e). Thus, though the winds were the strongest of all the seasons, it was unable to break the stratification and initiate wind-driven mixing to deepen the mixed layer. However, the shallow MLD seen around Sri Lanka, irrespective of the excess evaporation (Fig. A8), was not driven by the thermo-haline stratification but due to the positive wind stress curl (yellow broken counters in Fig. 5a–c). The positive wind

BGD
10, 16405–16452, 2013

cc BY

stress curl was seen developing in May which peaks in June and collapses by September (Fig. A7). This positive wind stress curl drives an upward Ekman pumping and this led to the observed shallow mixed layer around Sri Lanka. The band of deep mixed layer seen extending from the southwestern region of the study area into the central Bay was linked to the advection of high salinity waters from the Arabian Sea. An examination of SSS showed progressive advection of high salinity waters from the Arabian Sea into the central Bay during summer monsoon (Fig. A3). This high salinity waters reduced the upper ocean stratification as could be inferred from the stability parameter (Fig. 5e). Thus, the strong winds of the summer monsoon combined with the less stratified upper ocean due to the intrusion of high salinity waters from the Arabian Sea were able to drive strong wind-driven mixing. This led to the formation of deep MLD in summer. In addition to this, the negative wind stress curl in the central and western Bay also contributed to the observed deep MLD.

3.3 Fall intermonsoon

As the summer monsoon tapers off and the fall intermonsoon sets in, the shallow MLD region in the northern Bay, which was confined to north of 18° N, was seen extending southward and eastward, while southern part of the Bay showed deep mixed layer (Fig. 6). This could be explained in the context of changing atmospheric forcing from summer monsoon to fall intermonsoon. The short wave radiation as well as net heat flux showed a secondary heating of the upper ocean during fall intermonsoon (Figs. A4 and A5) and accordingly the SST was in excess of 29 °C in October (Fig. A2). Though the *E*-*P* showed a rapidly decreasing precipitation (Fig. A8) during this period, the surface salinity in contrast showed a progressive decrease from that of summer monsoon (Fig. A3). In addition, the low salinity waters also showed a further southward extension. This indicated that the shallow MLD in the northern Bay and its further southward extension was linked to the presence of low salinity waters and its southward advection. As seen from the data, the river discharge was dominant during July to October and hence the low salinity of the surface water was the manifestation of the river influence.

BGD
10, 16405–16452, 2013

cc BY

With the setting in of the fall intermonsoon, the winds over the Bay showed a drastic reduction in their speed in the north (Fig. A6). However, strong winds still persisted in the southern Bay. Thus, the deep MLD in the southern Bay was driven by a combination of comparatively high wind speed and the presence of high salinity waters (Fig. A3) both of which destabilized the water column.

3.4 Winter monsoon

The winter monsoon, in general, showed comparatively deep MLD (~ 30–40 m) all over the Bay except in the north and eastern Bay (Fig. 7). The shallow MLD (~ 5–15 m) in the north and eastern Bay could be understood in the context of the presence of low salinity waters (< 32 psu) during November–December (Fig. A3) and associated strong stratification. As the winter progressed, the E-P showed a net evaporation in most parts of the Bay (Fig. A8) while the region of low salinity waters were confined to the northern part during January–February. The shallow MLD observed near the Sumatra coast in January was driven by the strengthened positive wind stress curl (Fig. 7c) and the associated upward Ekman pumping. The deep MLD in the rest of the Bay was related to the weak stratification that occurred in the Bay during winter as could be inferred from the vertical structure of the stability parameter in the upper 40 m (Fig. 7e). The wind speed, which showed a secondary peak in winter (Fig. A6) were able to initiate deeper wind-mixing as the stratification of the water column was the weakest.

3.5 Role of Rossby waves

In order to understand the role of Rossby waves in regulating the MLD the time-longitude plot of sea-level anomaly along 16° N latitude was analyzed. For this purpose the monthly mean climatology of sea-level anomaly was computed from the monthly mean sea-level anomaly data for the period 1992 to 2006.

The time-longitude plot of sea-level anomaly along 16° N showed alternate bands of positive and negative anomalies with sloping counters having annual periodicity

BGD
10, 16405–16452, 2013

CC BY

(Fig. 8). These are the signature of westward propagating Rossby waves with positive sea-level anomaly during summer and negative during winter. In summer the central and eastern region showed the highest positive sea-level anomaly and this again contributed to the observed deep MLD in the southern Bay in addition to the reduction in stratification due to the intrusion of high salinity waters from the Arabian Sea.

3.6 Nitrate and chlorophyll

Having examined the seasonal cycle of basin-scale mixed layer variability, it is important to analyze the water-column nitrate and chlorophyll to understand how they respond to the changes in the MLD. Towards this, the nitrate and chlorophyll *a* at 10, 20, 50, and 100 m were analyzed and presented below. Surface values are not presented since the nitrate concentrations are generally in the undetectable levels. Only three seasons namely spring intermonsoon, summer monsoon and winter monsoon were considered as data in the fall intermonsoon was very few as mentioned in Sect. 2.2. In addition, the satellite derived chlorophyll pigment concentrations were also analyzed during the four seasons to decipher the seasonal cycle.

3.6.1 Spring intermonsoon

The nitrate concentrations at 10 m in most part of the basin during spring intermonsoon was very low ~0.5 µM (Fig. 9a). Along the northern and western Bay a high concentration was seen with the values in excess of 1 µM. A large patch in the central Bay also showed nitrate concentrations in the range of 1 to 1.5 µM. At 20 m, high nitrate concentrations in the range of 1 to 2 µM were seen along the western and northeastern boundary. The highest concentration of 3 µM was noticed north of Sri Lanka as a patch extending eastward (Fig. 9b). Similarly, two more patches of high nitrate concentration were seen south of Sri Lanka and southeastern Bay respectively. The distribution pattern at 50 m depth was similar to that of 20 m, but concentration levels were much higher ranging between 2 to 12 µM (Fig. 9c). At 100 m depth nitrate concen-

BGD
10, 16405–16452, 2013

CC BY

tration showed several eddy-like mesoscale variability and the values varied between 8 and 24 µM (Fig. 9d).

The chlorophyll *a* concentration at 10 m during spring intermonsoon was, in general, less than 0.2 mg m^{-3} except near the southern tip of India and along parts of the western and eastern boundary (Fig. 10a). The region between 91 to 98° E and 4 to 10° N also showed highest chlorophyll *a* concentrations with maximum value of 0.7 mg m^{-3}. In the central and southern Bay the chlorophyll *a* was least and the value varied between 0.1–0.2 mg m^{-3}. Though the spatial distribution pattern of chlorophyll *a* at 20 and 50 m (Fig. 10b, c) was similar to that of 10 m, the values showed an increase. The value varied between 0.2–1.0 mg m^{-3}. At 100 m the chlorophyll *a* concentrations in the entire Bay was less than 0.2 mg m^{-3} except in the southeastern Bay where it showed an increase from 0.2 to 0.7 mg m^{-3} (Fig. 10d).

3.6.2 Summer monsoon

The salient feature of nitrate distribution in the upper 20 m during summer was the presence of high concentrations in the Indo-Sri Lankan region where the highest values were 6 µM near peninsular India and 3 µM off Sri Lanka (Fig. 11a, b). Another region of high concentration was in the northern Bay. The rest of the Bay had nitrate concentrations less than 0.5 µM. At 50 and 100 m the eddy-like mesoscale patterns were prominently seen (Fig. 11c, d).

The spatial distribution of chlorophyll *a* at 10 m showed highest concentration of 0.5 mg m^{-3}in the northern Bay and also along the western boundary (Fig. 12a). However, the pattern was completely different at 20 m and region of highest chlorophyll *a* with a value of ~2 mg m^{-3} was seen in the Indo-Sri Lanka region (Fig. 12b). In the rest of the Bay the chlorophyll *a* concentration was less than 0.2 mg m^{-3}. The low chlorophyll *a* in the northern Bay in spite of the high nitrate concentration indicates the possible light limitation as the river runoff brings large amount of suspended load into the northern Bay. Though this pattern of high values near Indo-Sri Lanka region and

cc BY

very low values in the rest of the Bay remained same up to 100 m, their magnitude showed a progressive decrease with depth (Fig. 12c, d).

3.6.3 Winter monsoon

The nitrate distribution at 10 and 20 m (Fig. 13a, b) during winter season showed very low concentrations in most parts of the Bay (< 0.2 µM), except the region off Sumatra. At 50 and 100 m the nitrate concentrations varied between 2 and 24 µM (Fig. 13c, d). The eddy-like mesoscale feature was discernible at these depths.

The chlorophyll *a* distribution in winter at 10 and 20 m was similar to spring inter-monsoon, with high values along the western and eastern parts of the Bay, low values (< 0.1 mg m^{-3}) in the rest of the Bay (Fig. 14a, b). At 50 m the chlorophyll *a* over the Bay varied between 0.1 to 0.3 mg m^{-3} except along the western boundary where it was more than 0.4 mg m^{-3} (Fig. 14c). At 100 m most of the Bay showed low chlorophyll *a* with concentrations of about 0.1 mg m^{-3}, except a patch near the southern part of the western Bay where the concentration was ∼ 0.5 mg m^{-3} (Fig. 14d).

3.7 Satellite-derived chlorophyll pigment concentrations

The satellite-derived chlorophyll pigment concentrations showed the least value during spring intermonsoon compared to the rest of the 3 seasons (Fig. 15). The pigment concentrations varied over a very narrow range of 0.1 to 0.2 mg m^{-3}, except in the head Bay and close to peninsular India and Sri Lanka where it marginally increased to 0.3 mg m^{-3} (Fig. 15a). The chlorophyll pigment concentrations during summer monsoon were the highest followed by the fall intermonsoon (Fig. 15b, c). The region of highest chlorophyll pigment concentration was located in a region encompassing the peninsular India and Sri Lanka and northern Bay. These patterns were comparable with the in situ concentrations seen in the earlier section. The northern Bay showed a maximum value of about 1 mg m^{-3}, while near the Indo-Sri Lanka region it varied between 0.5–10 mg m^{-3}. Note that the red band usually seen very close to the coast

BGD
10, 16405–16452, 2013

in the pigment concentration map is largely due to sediments and should be neglected. During winter the chlorophyll pigment concentration showed a further reduction from that of the fall intermonsoon with the values ranging between 0.1 to 0.3 mg m^{-3} in most parts of the Bay (Fig. 15d). However, close to the western and eastern boundary the values varied between 0.3 and 2.5 mg m^{-3}.

4 Summary and conclusion

The seasonal variability of mixed layer depth and the factors responsible for the observed variability were investigated using a suite of in situ as well as remote sensing data pertaining to ocean and atmospheric parameters. The mixed layer was shallowest during spring intermonsoon compared to the rest of the seasons. The shallow mixed layer in the northern Bay was driven by the strong thermo-haline stratification due to the peak heating by incoming short wave radiation and the presence of low salinity waters. The prevailing weak winds were unable to break the stratification to drive deep wind-mixing resulting in the formation of shallow mixed layer. In the southern Bay, however, the comparatively weaker stratification and the prevalence of moderate winds were able to initiate greater wind-mixing leading to the formation of comparatively deeper mixed layer. During summer, in spite of the fact that the basin-wide winds were the strongest, the northern Bay continued to house shallow mixed layer. The excess precipitation over evaporation combined with the fresh water influx from the rivers adjoining the Bay of Bengal contributed towards freshening of the surface waters of the northern Bay. The resulting strong haline stratification inhibited deep mixing by the strongest winds. The shallow mixed layer in the region encompassing the southern part of the peninsular India and Sri Lanka was due to the upwelling associated with positive wind stress curl, while the band of deep mixed layer extending from southwestern region into the central Bay was associated with the advection of high salinity waters from the Arabian Sea. In addition, the presence of high sea-level anomaly in the central and eastern part of the southern Bay of Bengal during summer associated with the propagating Rossby wave

BGD
10, 16405–16452, 2013

CC BY

of annual periodicity also contributed towards the deep mixed layer in the southern Bay. During fall intermonsoon, the south ward extension of the shallow mixed layer resulted from the advection of the low salinity waters from the northern Bay combined with the secondary heating by incoming short wave radiation. The basin-wide deep mixed layer during winter was due to the basin-wide decrease in the upper water column stratification brought about by a combination of reduced short wave radiation, increase in salinity and comparatively stronger winds.

The seasonal variability of the nitrate and chlorophyll *a* showed that in the upper layer the concentration of nitrate was the least during spring intermonsoon compared to the rest of the seasons. The warm and strongly stratified upper ocean during spring intermonsoon with week winds led to shallow mixed layer making it highly oligotrophic. Consistent with this, the chlorophyll *a* concentrations, both in situ as well as satellite-derived, were also the least of all the seasons. In contrast, the nitrate concentrations during summer monsoon were the highest in the region encompassing the southern part of the peninsular India and Sri Lanka driven by the wind stress curl. Accordingly, the chlorophyll *a* concentrations were also the highest. In the northern Bay though the nitrate concentrations were high, a concomitant increase was not seen in the chlorophyll *a* indicating the possible light limitation. In fall intermonsoon, though the nutrient data and in situ chlorophyll *a* data were not available, the satellite-derived chlorophyll pigment concentrations showed pattern similar to that of summer monsoon with a reduced concentration indicating the tapering effect of summer monsoon. In winter, though the nitrate concentrations were very low in the upper layers the chlorophyll *a* concentrations were comparatively high along the western boundary indicating a mismatch between them. It is to be noted that the number of chlorophyll *a* data for any given season is much less in comparison with the nitrate data. Also the spatial coverage of chlorophyll *a* data also is less adequate compared to nitrate data. Hence it is quite possible that this data were unable to resolve all the characteristics of the seasonal variability. Nevertheless, the salient features such as summer monsoon high concentrations in the northern Bay as well as near the Indo-Sri Lanka region, the comparatively

BGD
10, 16405–16452, 2013

CC BY

high concentrations along the western boundary and the lowest concentrations during spring intermonsooon were all captured. Thus, we see a strong coupling between the seasonal cycle of mixed layer depth and the seasonally altering physical processes which intern is coupled to the chlorophyll pigment concentrations in the upper ocean.

Acknowledgements. Authors are thankful to Direction, CSIR-NIO, Goa and Council of Scientific and Industrial Research (CSIR), New Delhi for all the support and encouragement. We also acknowledge the help rendered by P. M. Muraleedharan, late G. Nampoothiri and M. Nuncio in data collection. This work was supported by Ministry of earth sciences (MoES), New Delhi under the programme BOB Process studies (BOBPS). J. Narvekar acknowledges Department of Science and Technology, New Delhi for the fellowship. This is NIO contribution number xxxxx.

References

Bathen, K. H.: On the seasonal changes in the depth of mixed layer in the north Pacific Ocean, J. Geophys. Res., 77, 7138–7150, 1972.

Boyer, T. P., Antonov, J. I.,Garcia, H., Johnson, D. R., Locarnini, R. A., Mishonov, A. V., Pitcher, M. T., Baranova, O. K., and Smolyar, I.: World Ocean Database 2005, Chapter 1: Introduction, NOAA Atlas NESDIS 60, Ed. S. Levitus, US Government Printing Office, Washington, D.C., 182 pp., 2006.

Brainerd, K. E. and Gregg, M. C.: Surface mixed and mixing layer depths, Deep-Sea Res. I., 42, 1521–1543, 1995.

Colburn, J. G.: The thermal structure of the Indian Ocean, International Indian Ocean Expedition Monographs 2, University Press of Hawaii, Honolulu, 1975.

de Boyer Montegut, C., Mignot. J., Lazar, A., and Cravatte, S.: Control of salinity on the mixed layer depth in the world ocean: 1. General description, J. Geophys. Res., 112, C06011, doi:10.1029/2006JC003953, 2007.

Gopalakrishna, V. V., Sadhuram, Y., and Ramesh Babu, V.: Variability of mixed layer depth in the northern Indian Ocean during 1977 and 1979 summer monsoon seasons, Indian J. Mar. Sci., 17, 258–264, 1988.

Hastenrath, S. and Greischar, L. L.: Climatic atlas of the Indian Ocean, part-III, Upper-Ocean structure, USA: The University of Wisconsin Press, 247 pp., 1989.

CC BY

Han, W., McCreary, J. P., and Kohler, K. E.: Influence of precipitation minus evaporation and Bay of Bengal rivers on dynamics, thermodynamics, and mixed layer physics in the upper Indian Ocean, J. Geophys. Res., 106, 6895–6916, 2001.

Kara, A. B., Rochford, P. A., and Hurburt, H. E.: Mixed layer depth variability over the global ocean, J. Geophys. Res., 108, 3079, doi:10.1029/2000JC000736, 2003.

Keerthi, M. G., Lengaigne, M. Vialard, J., de Boyer Montégut, C., and Muraleedharan, P. M.: Interannual variability of the Tropical Indian Ocean mixed layer depth, Clim. Dynam., 40, 743–759, 2012.

Levitus, S.: Climatological Atlas of the World Ocean, NOAA Professional paper 13, National Oceanic and Atmospheric Administration, Rockville Md, 173 pp., 1982.

Lukas, R. and Lindstrom, E.: The mixed layer of the western equatorial Pacific Ocean, J. Geophys. Res., 96, 3343–3357, 1991.

Lukas, R. and Lindstrom, E.: The mixed layer of the western equatorial Pacific Ocean, J. Geophys. Res., 96, 3343–3357, 1991.

Monterey, G. and Levitus, S.: Seasonal variability of mixed layer depth for the world ocean, NOAA atlas NESDIS 14, US Gov. Printing Office, Washington, D.C., 87 figures & 96 pp., 1997.

Narvekar, J. and Prasanna Kumar, S.: Seasonal variability of the mixed layer in the central Bay of Bengal and associated changes in nutrients and chlorophyll, Deep-Sea Res. I, 53, 820–835, 2006.

Pond, S. and Pickard, G. L.: Introductory dynamical oceanography, Pergamon Press, New York, 241 pp., 1983.

Prasad, T. G.: A comparison of mixed layer dynamics between the Arabian Sea and the Bay of Bengal: One dimensional model results, J. Geophys. Res., 109, C03035, doi:10.1029/2003JC002000, 2004.

Rao, R. R., Molinari, R. L., and Festa, J. F.: Evolution of the climatological near-surface thermal structure of the tropical Indian Ocean: Description of mean monthly mixed-layer depth and sea-surface temperature, surface-current and surface meteorological fields, J. Geophys. Res., 94, 1081–10815, 1989.

Rao, R. R., Molinari, R. L., and Festa, J. F.: Surface meteorological and near surface oceanographic atlas of the tropical Indian Ocean, NOAA Technical Memorandum ERLAOML, 69, 59 pp., 1991.

CC BY

Rao, R. R. and Sivakumar, R.: Seasonal variability of near-surface thermal structure and heat budget of the mixed layer of the tropical Indian ocean from a new global ocean temperature climatology, J. Geophys. Res., 105, 995–1016, 2000.

Rao, R. R. and Sivakumar, R.: Seasonal variability of sea surface salinity and salt budget of the mixed layer of the north Indian Ocean, J. Geophys. Res., 108, 3009, doi:10.1029/2001JC000907, 2003.

Robinson, M. K., Baur, R. A., and Schroeder, E. H.: Atlas of North Atlantic-Indian Ocean monthly mean temperature and mean salinities of the surface layer, Naval Oceanographic Office Reference Publication 18, Department of the Navy, Washington, D.C, 203073, 213 pp., 1979.

Shenoi, S. S. C., Shankar, D., and Shetye, S. R.: Difference in heat budgets of the nearsurface Arabian Sea and Bay of Bengal: Implications for the summer monsoon, J. Geophys. Res., 107, 5-1–5-14, doi:10.1029/2000JC000679, 2002.

Schneider, N. and Muller, P.: The meridional and seasonal structures of the mixed layer depth and its diurnal amplitude observed during the Hawaii-to-Tahiti Shuttle Experiment, J. Phys. Oeanogr., 20, 1395–1404, 1990.

Sprintall, J. and Tomczak, M.: Evidence of barrier layer in the surface layer of the tropics, J. Geophys. Res., 97, 7305–7316, 1992.

Subramanian, V.: Sediment load of Indian Rivers, Cur. Sci., 64, 928–930, 1993.

UNESCO, Technical papers in marine science, United Nations Educational, Scientific and Cultural Organization, Paris, 192 pp., 1981.

Vinaychandran, P. N., Murthy, V. S. N., and Ramesh, B. V.: Observations on barrier layer formation in the Bay of Bengal during summer monsoon, J. Geophys. Res., 107, 8018, doi:10:1029/200JC000831, 2002.

Weller, R. A. and Farmer, D. M.: Dynamics of the ocean mixed layer, Oceans, 35, 46–55, 1992.

Wyrtki, K.: The thermal structure of the eastern Pacific Ocean, Dtsch. Hydrogr. Ze., Supplement A8, 6–84, 1964.

BGD
10, 16405–16452, 2013

Table 1. Total number of temperature and salinity profiles in the Bay of Bengal for each month from January to December.

Month	Total No. of Profiles
Jan	987
Feb	1079
Mar	733
Apr	769
May	856
Jun	750
Jul	1279
Aug	1302
Sep	996
Oct	890
Nov	920
Dec	1626

BGD
10, 16405–16452, 2013

CC BY

BGD

10, 16405–16452, 2013

Title Page
Abstract | Introduction
Conclusions | References
Tables | Figures
◀| |▶
◀ ▶
Back | Close
Full Screen / Esc
Printer-friendly Version
Interactive Discussion

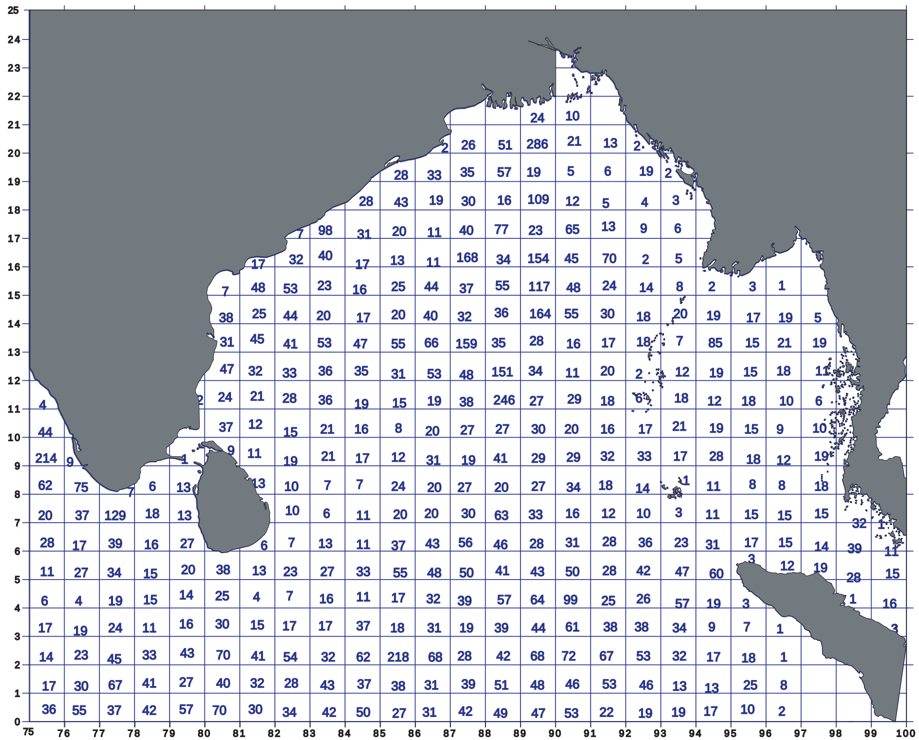

Fig. 1. Spatial distribution of total number of temperature and salinity profiles available on a 1° latitude by 1° longitude grids.

CC BY

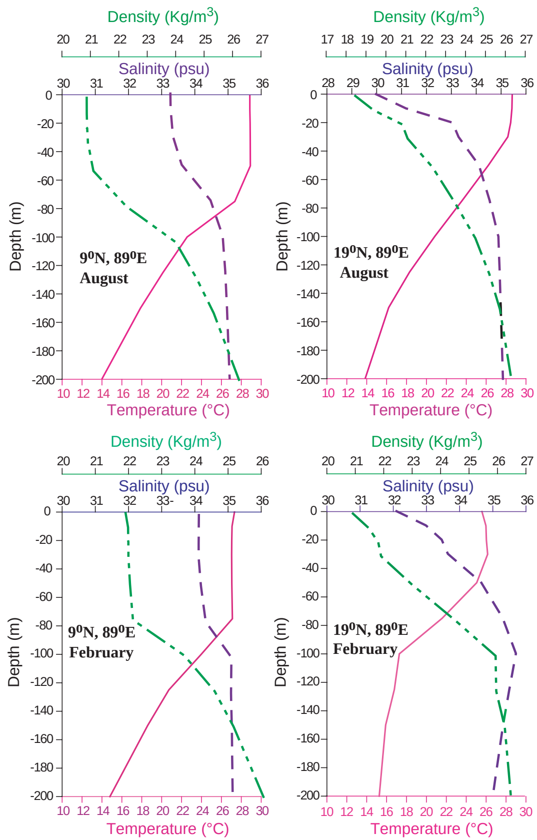

Fig. 2. Vertical profiles of temperature, salinity and density (sigma-*t*) at two locations representing the northern (19° N, 89° E) and southern (9° N, 89° E) Bay of Bengal during February (winter) and August (summer).

BGD
10, 16405–16452, 2013

CC BY

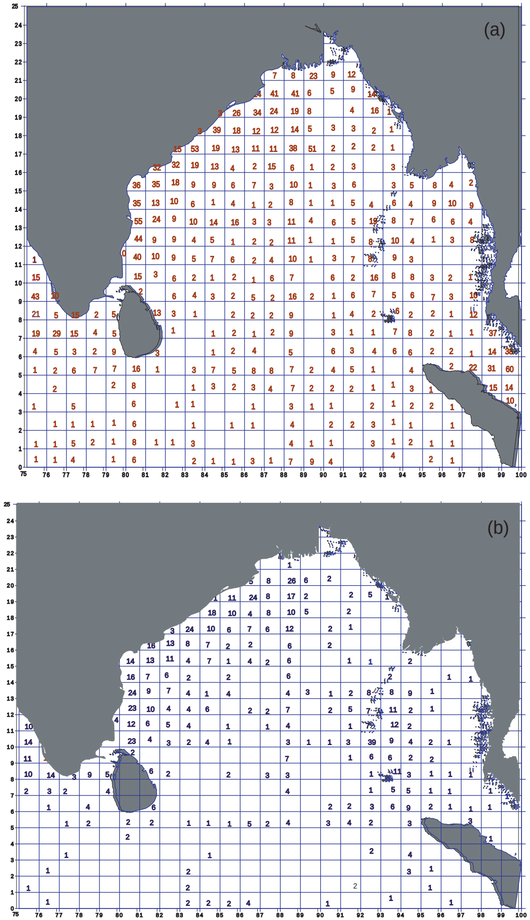

Fig. 3. Total number of profiles of **(a)** nitrate and **(b)** chlorophyll *a* available at each of the 1° latitude × 1° longitude grid.

BGD
10, 16405–16452, 2013

J. Narvekar and
S. Prasanna Kumar

cc BY

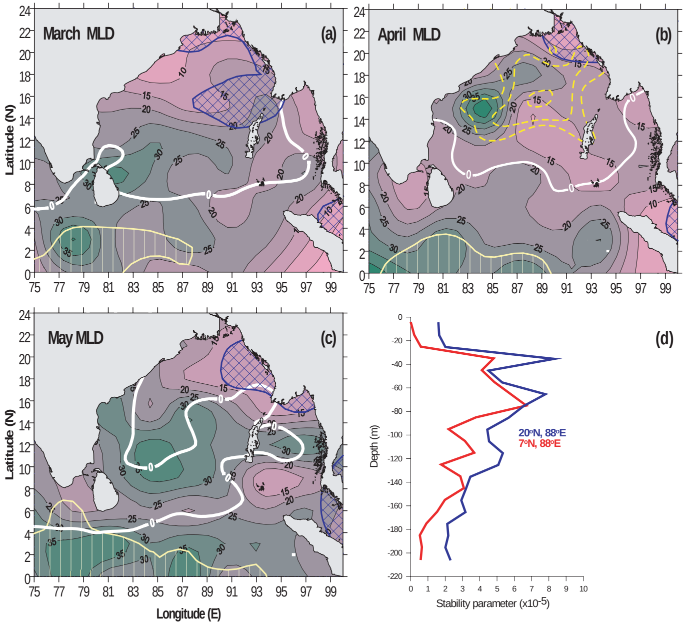

Fig. 4. Monthly mean climatology of mixed layer depth (m) in the Bay of Bengal during spring intermonsoon **(a)** March, **(b)** April and **(c)** May, and **(d)** vertical profiles of upper ocean stability parameter (E, m^{-1}) at 20° N, 88° E (blue line) and 7° N, 88° E (red line) in April. In **(a–c)** the blue cross-hatch represents the region where salinity is less than 32 psu, while vertical lines within the thin yellow solid line represent the region where the salinity is greater than 34.5 psu. The thick broad white line indicates the zero wind stress curl and the region south of it (equator ward) have positive wind stress curl. The yellow broken contours in **(b)** indicate the negative wind stress curl (-10 to -20×10^{-8} Pascal m^{-1}) with increasing magnitude towards the centre.

BGD
10, 16405–16452, 2013

CC BY

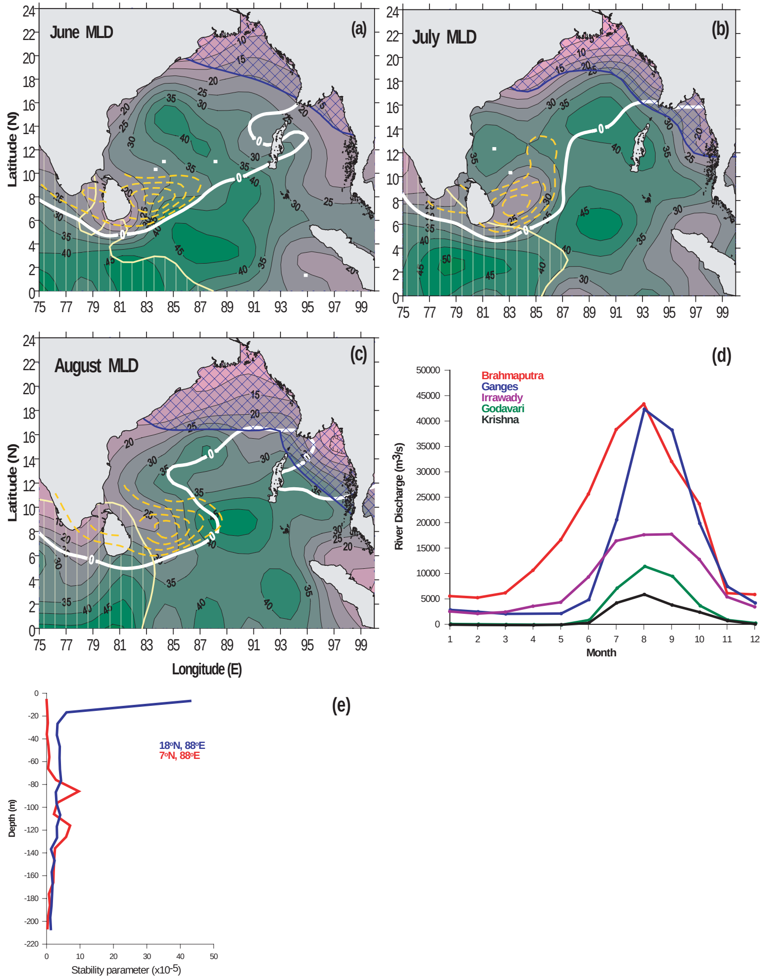

BGD
10, 16405–16452, 2013

J. Narvekar and S. Prasanna Kumar

cc BY

Fig. 5. Monthly mean climatology of mixed layer depth (m) in the Bay of Bengal during summer **(a)** June, **(b)** July and **(c)** August, **(d)** monthly mean river discharge climatology of Ganges, Brahmaputra, Irrawady, Godavari and Krishna and **(e)** vertical profiles of upper ocean stability parameter (E, m^{-1}) at 18° N, 88° E (blue line) and 7° N, 88° E (red line) in the Bay of Bengal during July. In **(a–c)** the blue cross-hatch represents the region where salinity is less than 32 psu, while vertical lines within the thin yellow solid line represent the region where the salinity is greater than 34.5 psu. The thick broad white line indicates the zero wind stress curl and the region south of it (equator ward) have negative wind stress curl. The yellow broken contours indicate the positive wind stress curl (5 to 20×10^{-8} Pascal m^{-1}) with increasing magnitude towards the centre.

BGD
10, 16405–16452, 2013

CC BY

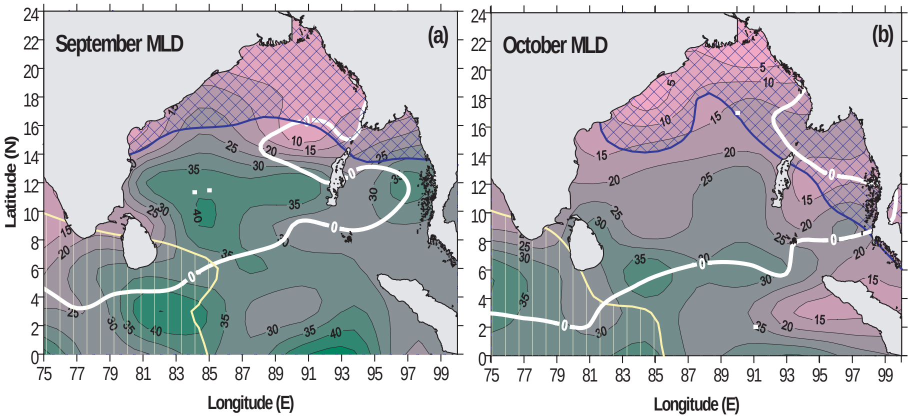

Fig. 6. Monthly mean climatology of mixed layer depth (m) in the Bay of Bengal during fall intermonsoon **(a)** September and **(b)** October. The blue cross-hatch represents the region where salinity is less than 32 psu, while vertical lines within the thin yellow solid line represent the region where the salinity is greater than 34.5 psu. The thick broad white line indicates the zero wind stress curl and the region south of it (equator ward) have positive wind stress curl.

BGD
10, 16405–16452, 2013

Mixed layer variability and chlorophyll *a* biomass

J. Narvekar and S. Prasanna Kumar

CC BY

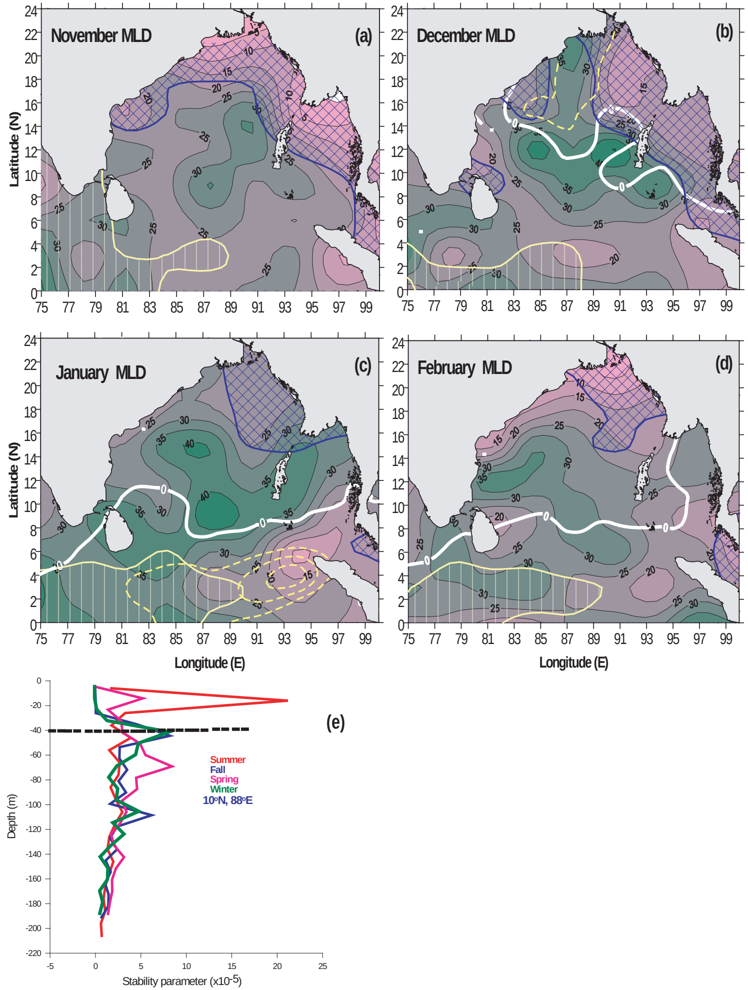

BGD
10, 16405–16452, 2013

CC BY

Fig. 7. Monthly mean climatology of mixed layer depth (m) in the Bay of Bengal during winter **(a)** November, **(b)** December, **(c)** January, and **(c)** February and **(e)** vertical profiles of upper ocean stability parameter (E, m^{-1}) at 10° N, 88° E. In **(a–d)** the blue cross-hatch represents the region where salinity is less than 32 psu, while vertical lines within the thin yellow solid line represent the region where the salinity is greater than 34.5 psu. The thick broad white line indicates the zero wind stress curl and the region south of it (equator ward) have positive wind stress curl. The yellow broken contours indicate the positive wind stress curl (5 to 20 × 10^{-8} Pascal m^{-1}) with increasing magnitude towards the centre.

BGD
10, 16405–16452, 2013

CC BY

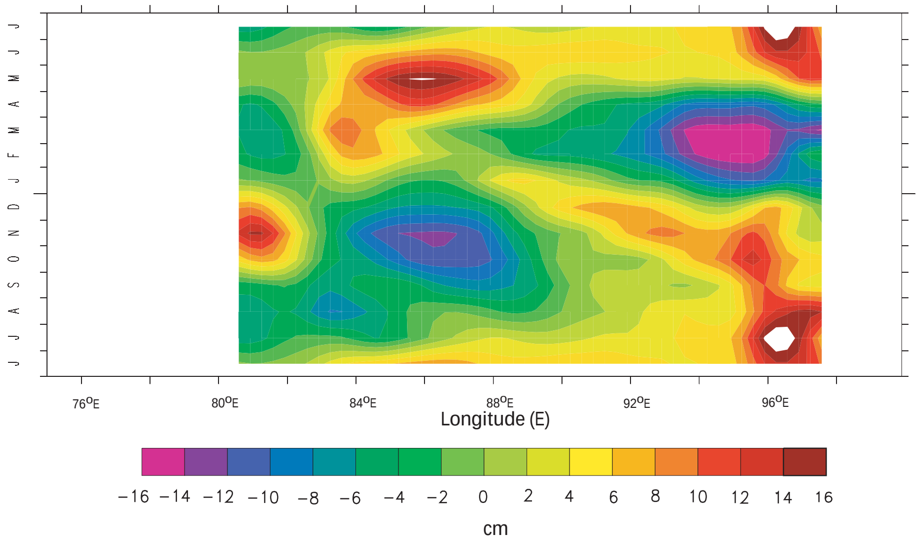

Fig. 8. Time-longitude plot of monthly mean sea-level anomaly climatology derived from merged sea-level anomalies of Topex/Poseidon and ERS 1/2 satellites along 16° N.

BGD
10, 16405–16452, 2013

Mixed layer variability and chlorophyll *a* biomass

J. Narvekar and S. Prasanna Kumar

CC BY

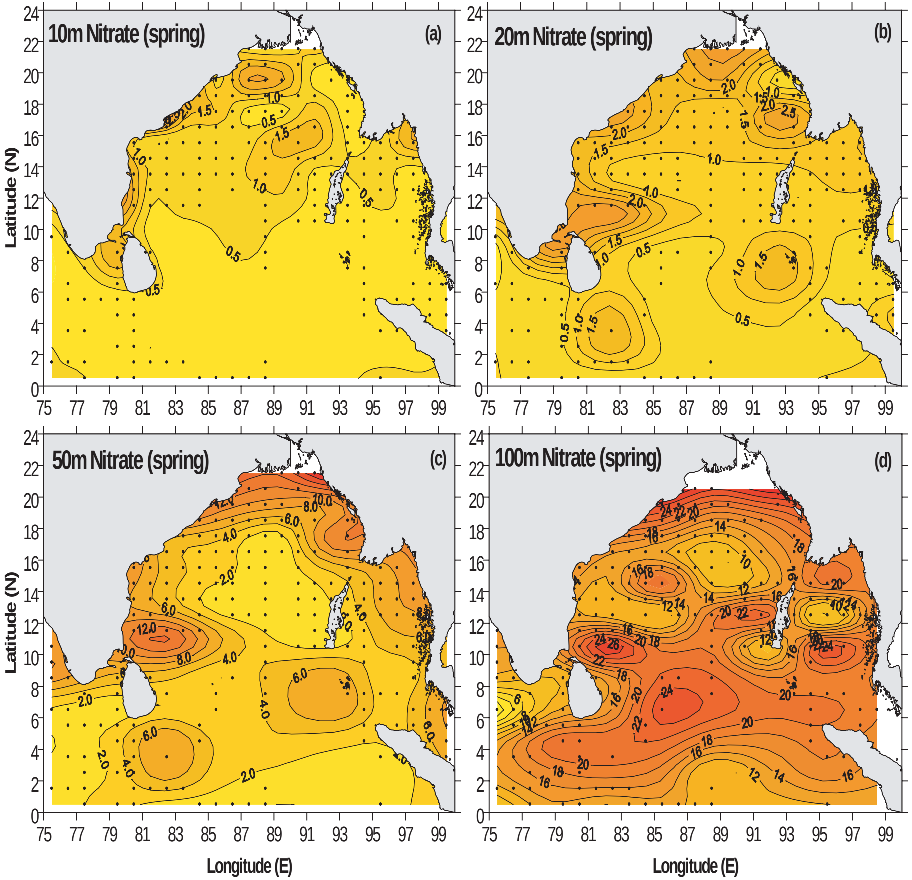

Fig. 9. Spatial distribution of nitrate (µM) at **(a)** 10 m, **(b)** 20 m, **(c)** 50 m, and **(d)** 100 m during spring intermonsoon. Note the change in contour interval in **(c)** and **(d)**.

CC BY

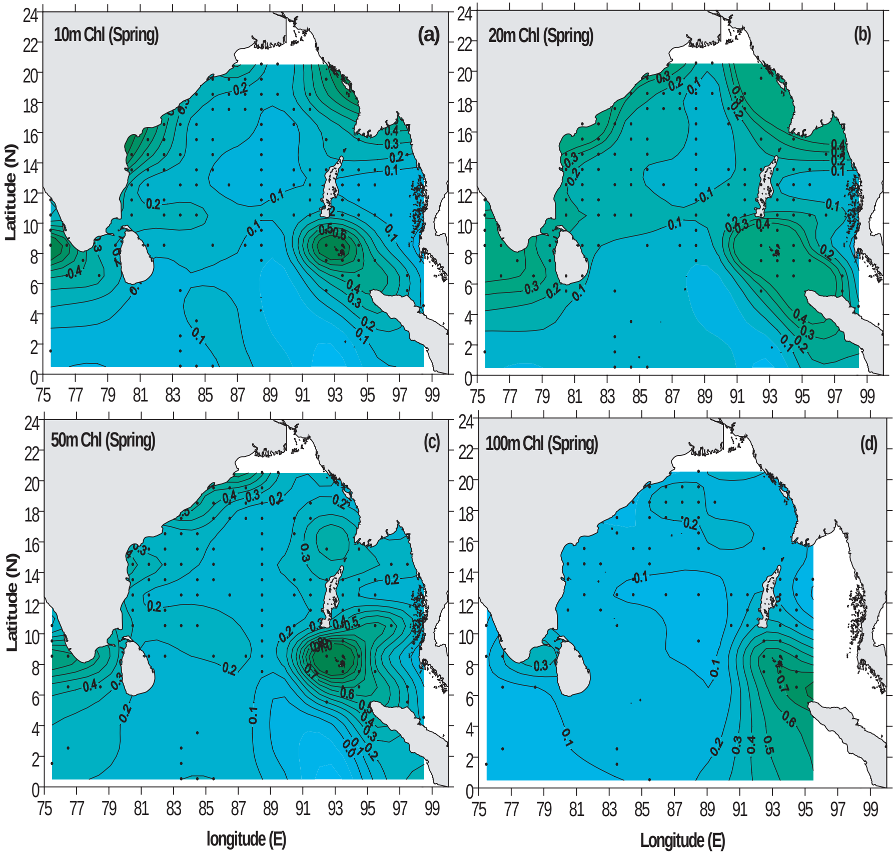

Fig. 10. Spatial distribution of chlorophyll *a* (mg m^{-3}) at **(a)** 10 m, **(b)** 20 m, **(c)** 50 m, and **(d)** 100 m during spring intermonsoon.

BGD
10, 16405–16452, 2013

Mixed layer variability and chlorophyll *a* biomass

J. Narvekar and S. Prasanna Kumar

CC BY

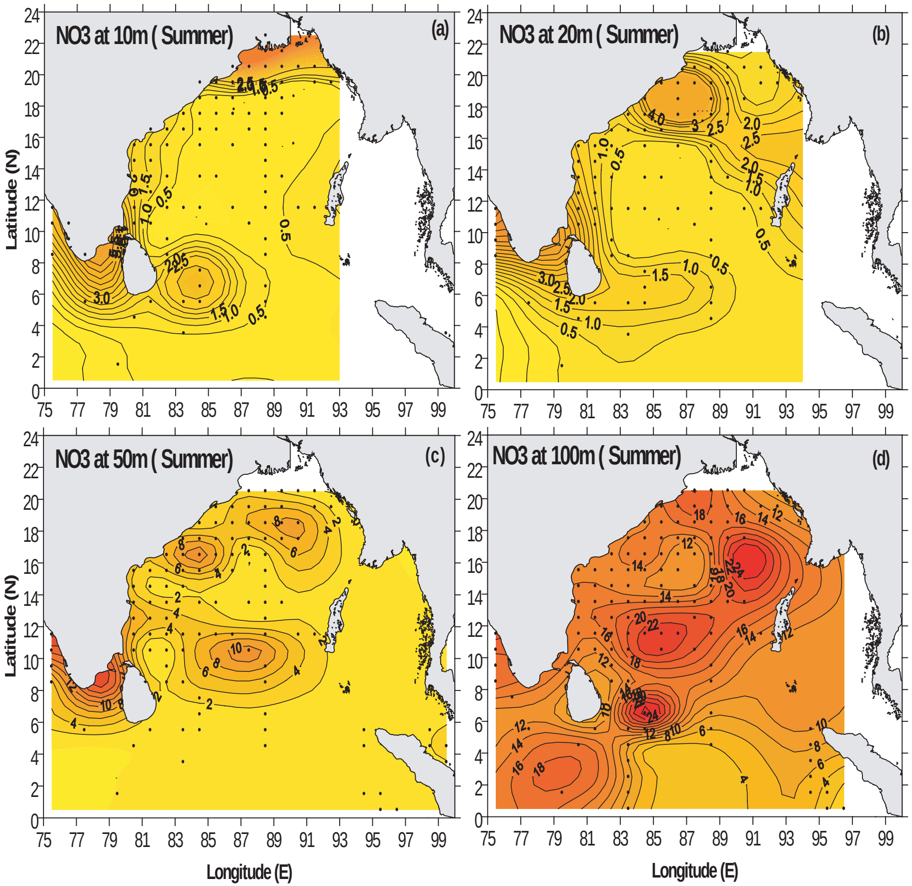

Fig. 11. Spatial distribution of nitrate (μM) at **(a)** 10 m, **(b)** 20 m, **(c)** 50 m, and **(d)** 100 m during summer monsoon. Note the change in contour interval in **(c)** and **(d)**.

BGD

10, 16405–16452, 2013

Mixed layer variability and chlorophyll *a* biomass

J. Narvekar and S. Prasanna Kumar

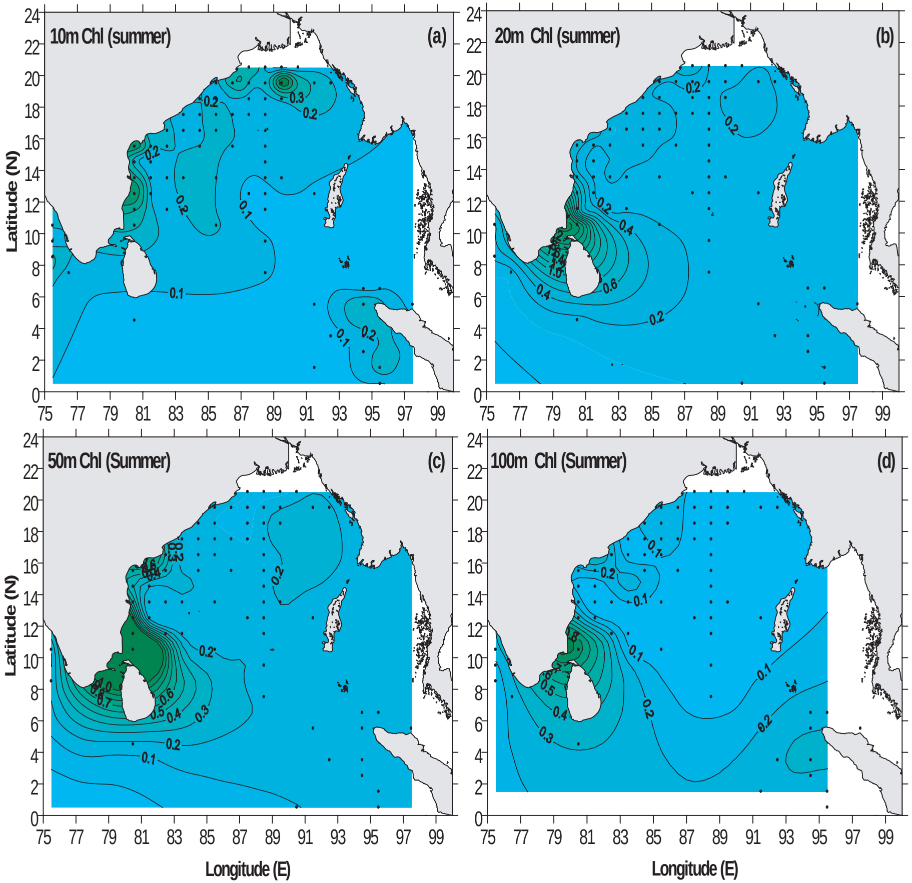

Fig. 12. Spatial distribution of chlorophyll *a* (mg m^{-3}) at **(a)** 10 m, **(b)** 20 m, **(c)** 50 m, and **(d)** 100 m during summer monsoon. Note the change in contour interval in **(b)**.

BGD

10, 16405–16452, 2013

Mixed layer variability and chlorophyll *a* biomass

J. Narvekar and S. Prasanna Kumar

CC BY

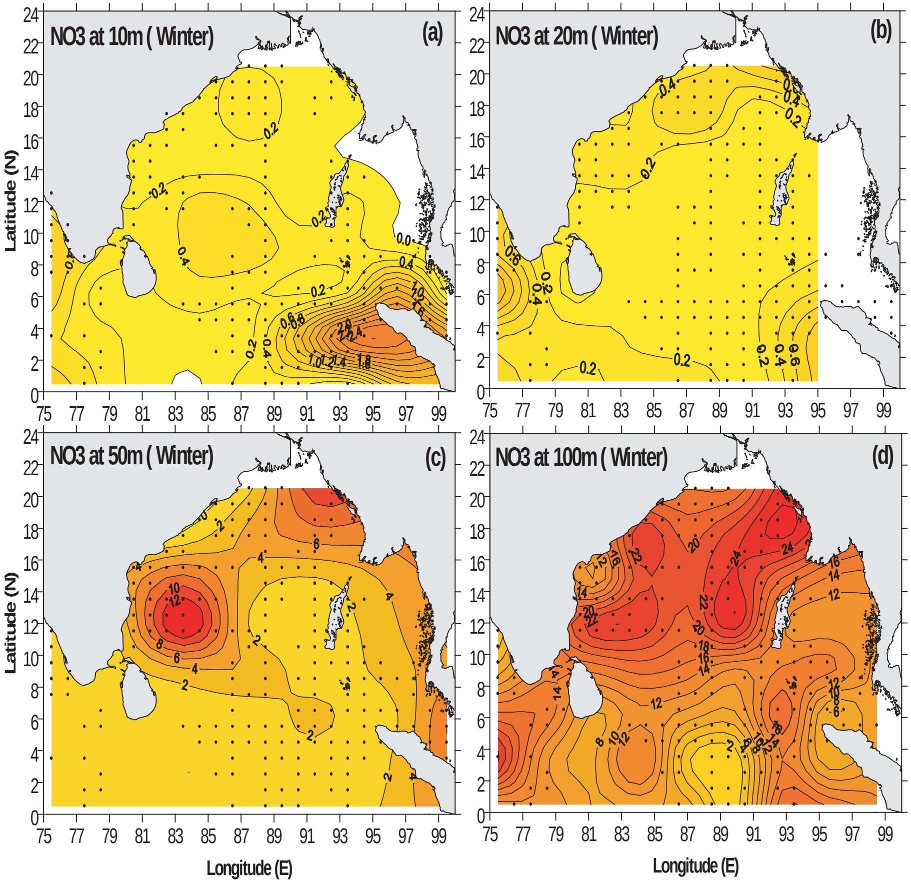

Fig. 13. Spatial distribution of nitrate (µM) at **(a)** 10 m, **(b)** 20 m, **(c)** 50 m, and **(d)** 100 m during winter monsoon. Note the change in contour interval in **(c)** and **(d)**.

BGD
10, 16405–16452, 2013

J. Narvekar and S. Prasanna Kumar

cc BY

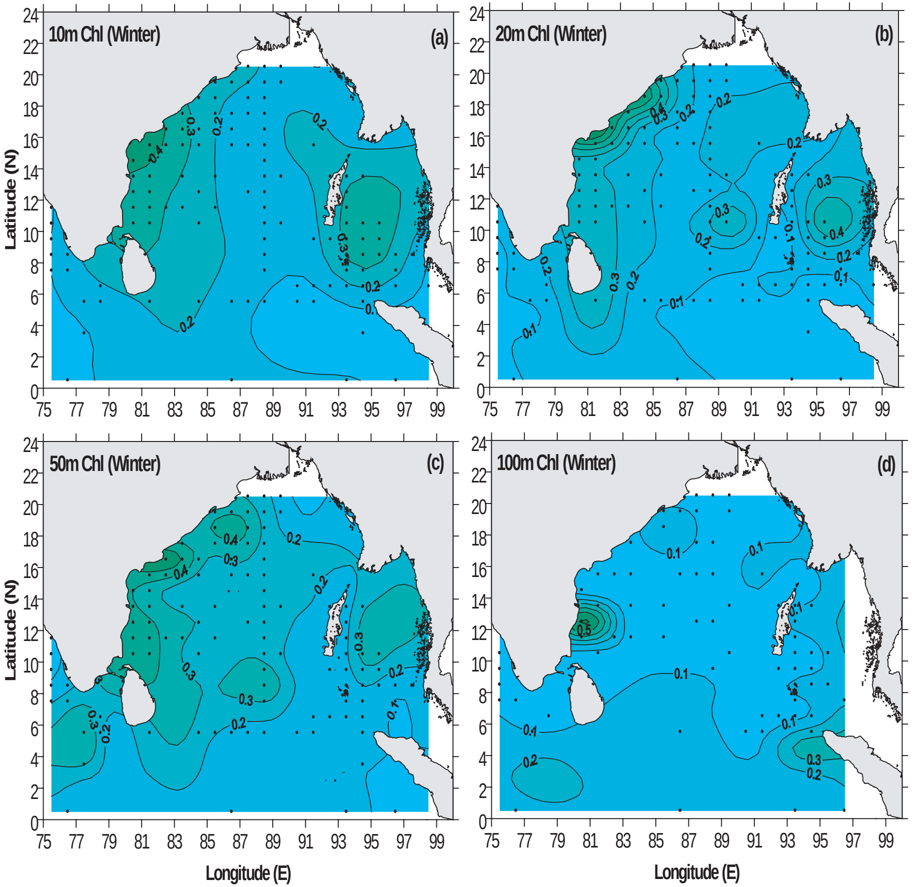

Fig. 14. Spatial distribution of chlorophyll *a* (mg m^{-3}) at **(a)** 10 m, **(b)** 20 m, **(c)** 50 m, and **(d)** 100 m during winter monsoon.

BGD
10, 16405–16452, 2013

Mixed layer variability and chlorophyll *a* biomass

J. Narvekar and S. Prasanna Kumar

Title Page
Abstract | Introduction
Conclusions | References
Tables | Figures
◀| |▶
◀ ▶
Back | Close
Full Screen / Esc
Printer-friendly Version
Interactive Discussion

CC BY

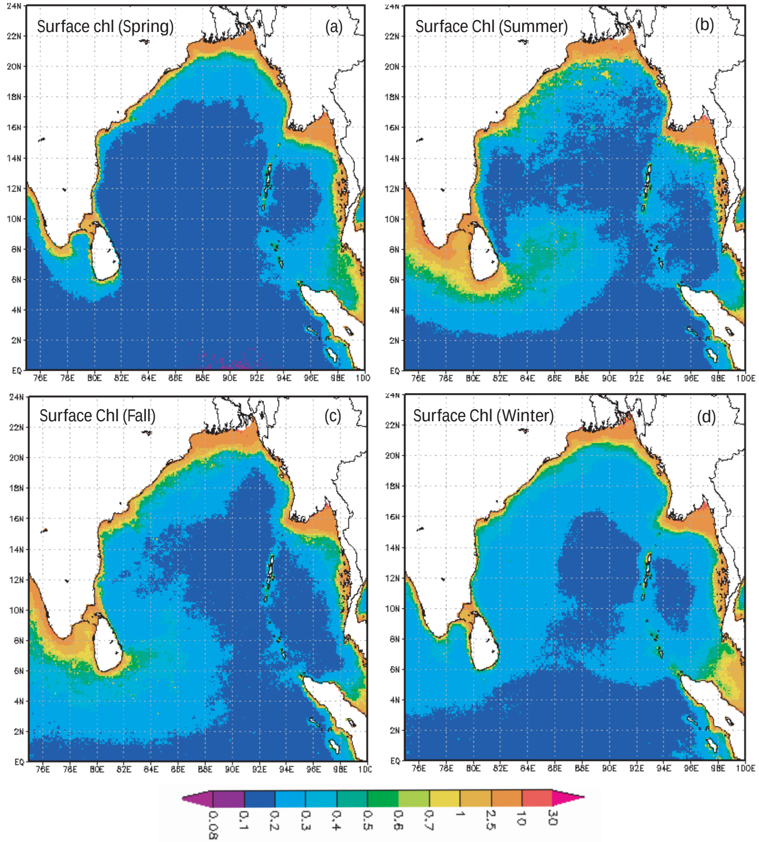

Fig. 15. Satellite-derived surface chlorophyll pigment concentrations (mg m^{-3}) in the Bay of Bengal during **(a)** spring intermonsoon, **(b)** summer, **(c)** fall intermonsoon and **(d)** winter monsoon.

BGD
10, 16405–16452, 2013

Mixed layer variability and chlorophyll *a* biomass

J. Narvekar and S. Prasanna Kumar

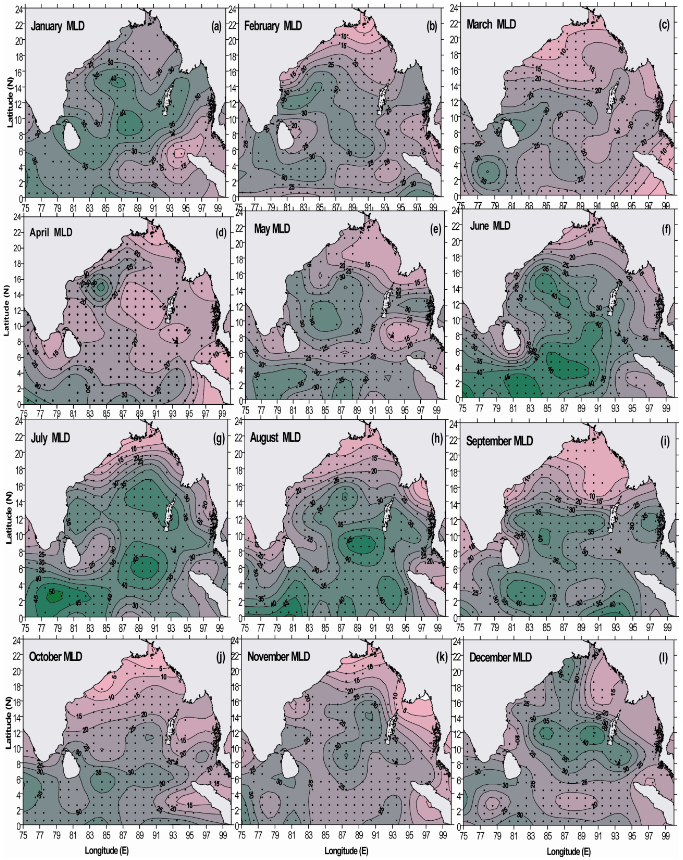

Fig. A1. Monthly mean climatology of mixed layer depth (MLD, m) from January to December.

BGD
10, 16405–16452, 2013

Mixed layer variability and chlorophyll *a* biomass

J. Narvekar and S. Prasanna Kumar

CC BY

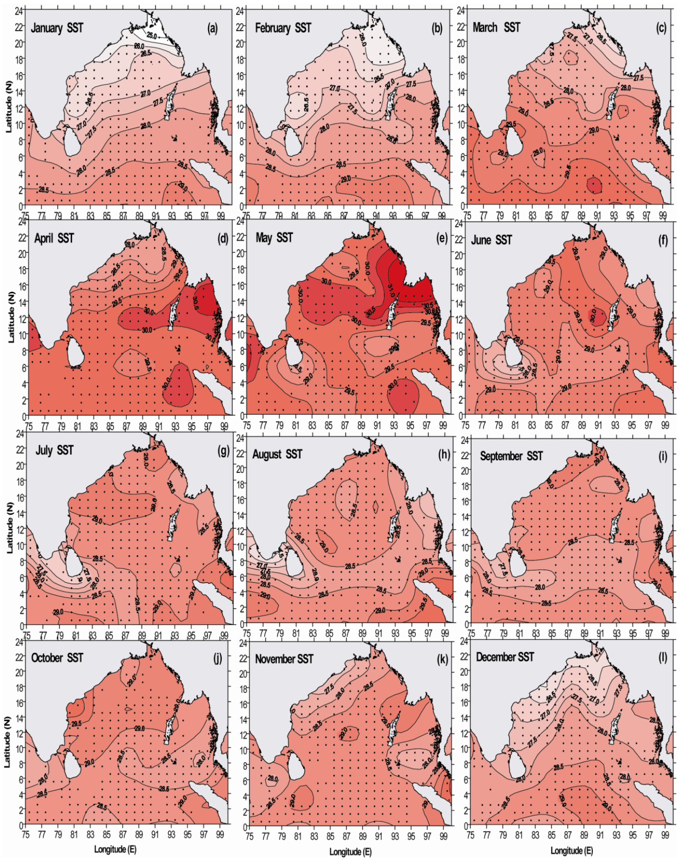

Fig. A2. Monthly mean climatology of sea surface temperature (SST, °C) from January to December.

BGD

10, 16405–16452, 2013

Mixed layer variability and chlorophyll *a* biomass

J. Narvekar and S. Prasanna Kumar

Title Page
Abstract | Introduction
Conclusions | References
Tables | Figures
◀| |▶
◀ ▶
Back | Close
Full Screen / Esc
Printer-friendly Version
Interactive Discussion

CC BY

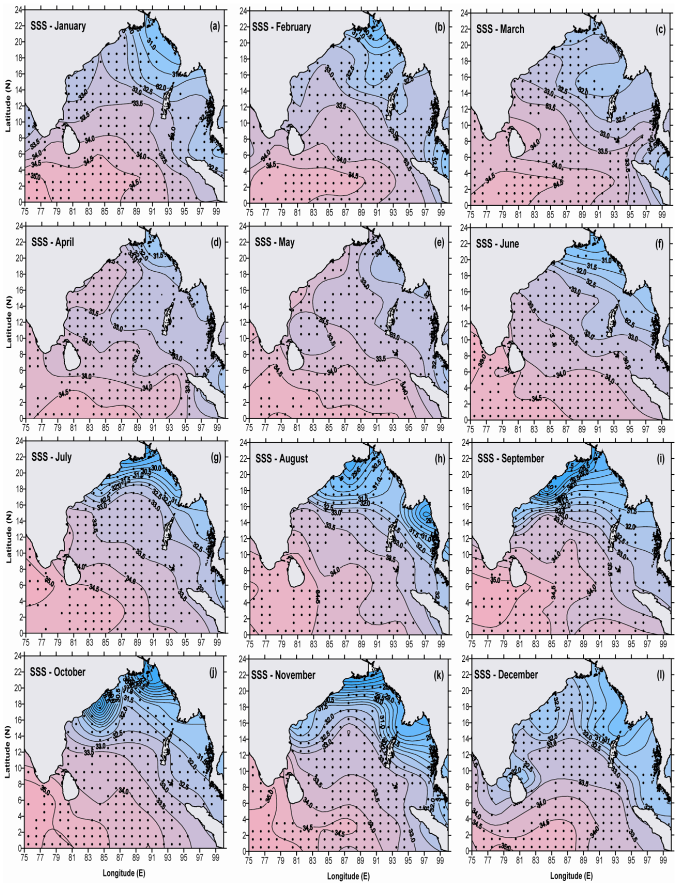

Fig. A3. Monthly mean climatology of sea surface salinity (SSS, psu) from January to December.

CC BY

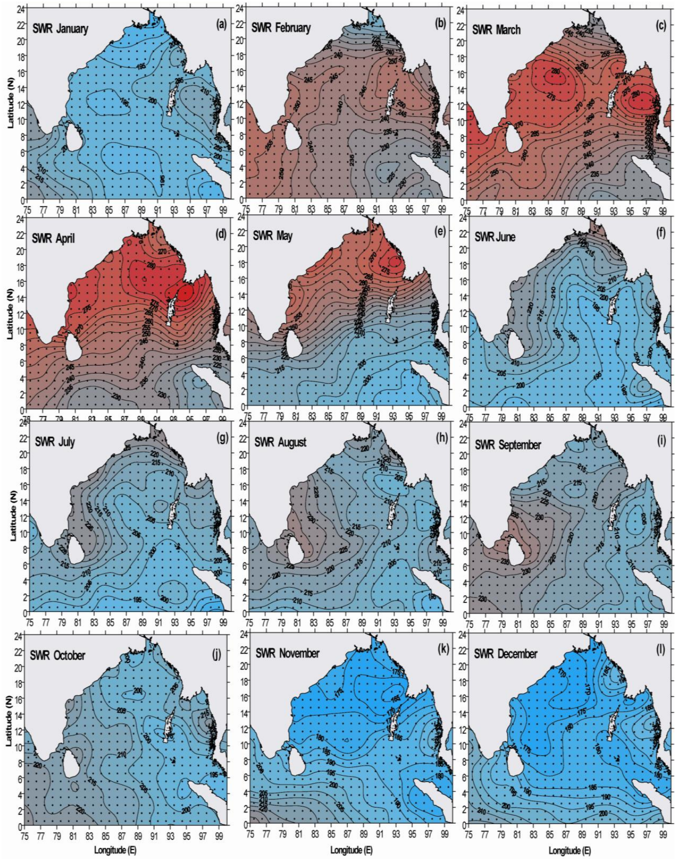

Fig. A4. Monthly mean climatology of incoming short wave radiation (SWR, $W\,m^{-2}$) from January to December.

BGD

10, 16405–16452, 2013

Mixed layer variability and chlorophyll *a* biomass

J. Narvekar and S. Prasanna Kumar

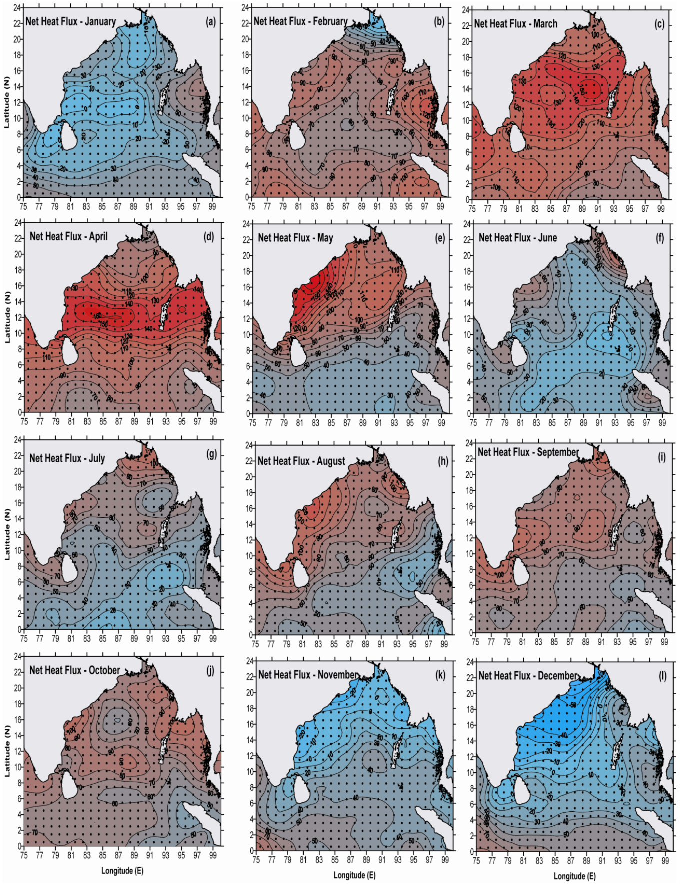

Fig. A5. Monthly mean climatology of net heat flux (NHF, $W\,m^{-2}$) from January to December.

BGD
10, 16405–16452, 2013

Mixed layer variability and chlorophyll *a* biomass

J. Narvekar and S. Prasanna Kumar

CC BY

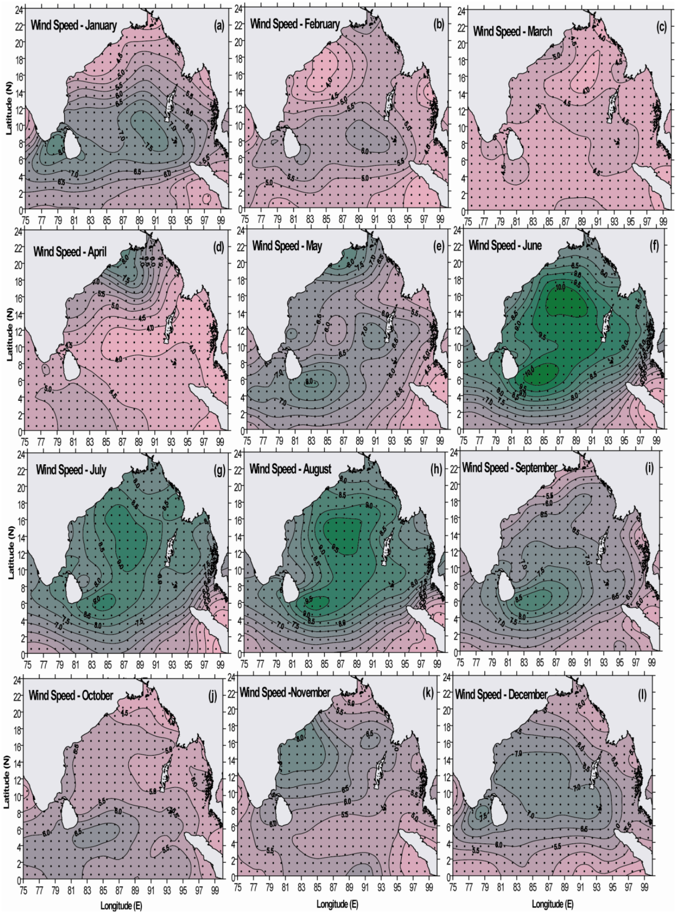

Fig. A6. Monthly mean climatology of wind speed (WS, m s^{-1}) from January to December.

BGD

10, 16405–16452, 2013

Mixed layer variability and chlorophyll *a* biomass

J. Narvekar and S. Prasanna Kumar

CC BY

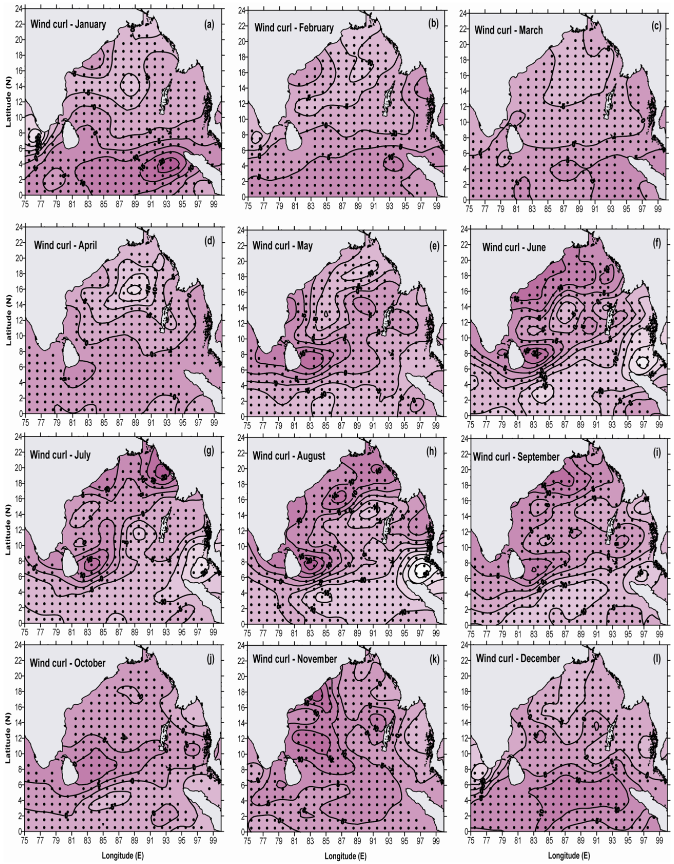

Fig. A7. Monthly mean climatology of wind-stress curl ($\times 10^{-8}$ Pascal m^{-1}) from January to December.

BGD
10, 16405–16452, 2013

Mixed layer variability and chlorophyll *a* biomass

J. Narvekar and S. Prasanna Kumar

CC BY

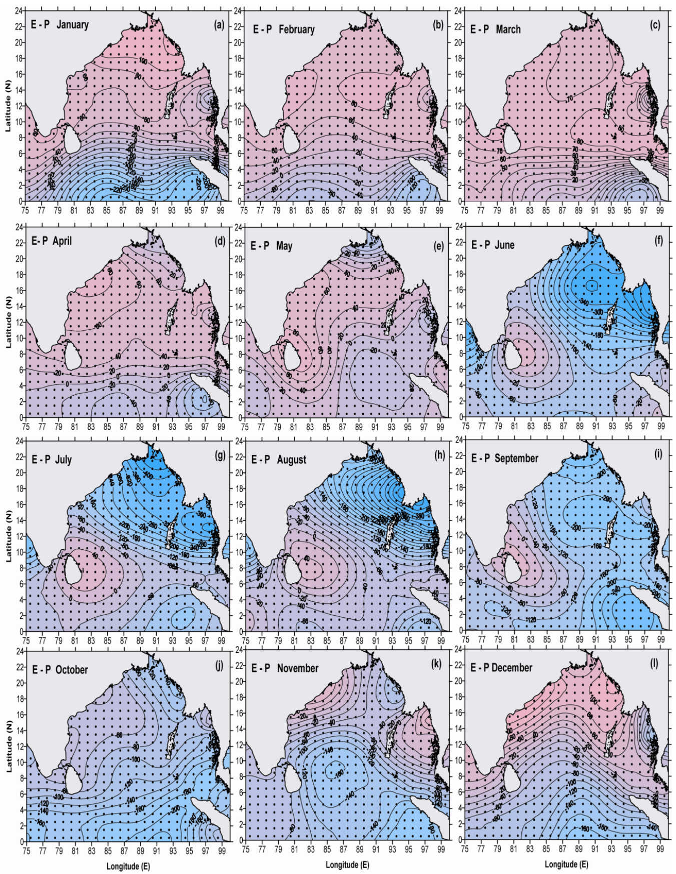

Fig. A8. Monthly mean climatology of fresh water flux (evaporation-precipitation) (*E-P*, mm month^{-1}) from January to December.

BGD

10, 16405–16452, 2013

Mixed layer variability and chlorophyll *a* biomass

J. Narvekar and S. Prasanna Kumar

Title Page
Abstract | Introduction
Conclusions | References
Tables | Figures
◀| |▶
◀ ▶
Back | Close
Full Screen / Esc
Printer-friendly Version
Interactive Discussion

CC BY